

Alterations in Cortical Thickness and Subcortical Volume are Associated With Neurological Symptoms and Neck Pain in Patients With Cervical Spondylosis

Davis C. Woodworth, BS*[‡]

Langston T. Holly, MD[§]

Emeran A. Mayer, MD[¶]

Noriko Salamon, MD, PhD*

Benjamin M. Ellingson,

PhD*^{‡||}

*Department of Radiological Sciences, David Geffen School of Medicine, University of California Los Angeles, Los Angeles, California; [‡]Department of Physics and Biology in Medicine, David Geffen School of Medicine, University of California Los Angeles, Los Angeles, California; [§]Department of Neurosurgery, David Geffen School of Medicine, University of California Los Angeles, Los Angeles, California; [¶]Gail and Gerald Oppenheimer Family Center for Neurobiology of Stress and Resilience, Departments of Medicine, Physiology, and Psychiatry, David Geffen School of Medicine, University of California Los Angeles, Los Angeles, California; ^{||}Department of Bioengineering, Henry Samueli School of Engineering and Applied Science, University of California Los Angeles, Los Angeles, California

Correspondence:

Benjamin M. Ellingson, PhD,
Associate Professor of Radiology,
Biomedical Physics, Bioengineering,
and Psychiatry,
Departments of Radiological Sciences
and Psychiatry,
David Geffen School of Medicine,
University of California Los Angeles,
924 Westwood Blvd, Suite 615,
Los Angeles, CA 90024.
E-mail: bellingson@mednet.ucla.edu

Received, July 26, 2017.

Accepted, February 7, 2018.

Published Online, March 14, 2018.

Copyright © 2018 by the
Congress of Neurological Surgeons

BACKGROUND: Advanced cervical spondylosis (CS) can cause structural damage to the spinal cord resulting in long-term neurological impairment including neck pain and motor weakness. We hypothesized long-term structural reorganization within the brain in patients with CS.

OBJECTIVE: To explore the associations between cortical thickness, subcortical volumes, neurological symptoms, and pain severity in CS patients with or without myelopathy and healthy controls (HCs).

METHODS: High-resolution T1-weighted structural magnetic resonance imaging (MRI) scans from 26 CS patients and 45 HCs were acquired. Cortical thickness and subcortical volumes were computed and compared to the modified Japanese Orthopedic Association (mJOA) and the Neck Disability Index (NDI) scores.

RESULTS: Cortical thinning within the superior frontal gyrus, anterior cingulate, precuneus, and reduction in putamen volume were associated with worsening neurological and pain symptoms. Among the strongest associations were cortical thickness within the left precuneus ($R^2 = 0.34$) and left and right putamen ($R^2 = 0.43, 0.47$, respectively) vs mJOA, and the left precuneus ($R^2 = 0.55$), insula ($R^2 = 0.57$), and right putamen ($R^2 = 0.54$) vs NDI ($P \leq .0001$ for all). Cortical thickness along Brodmann areas 3a, 4a, and 4p were also moderately associated with mJOA. Preliminary evidence also suggests that patients with CS may undergo cortical atrophy at a faster rate than HCs.

CONCLUSION: Patients with CS appear to exhibit cortical thinning and atrophy with worsening neurological and pain symptoms in specific brain regions associated with sensorimotor and pain processing.

KEY WORDS: Brain, Degenerative cervical myelopathy, Cervical spondylosis, Cortical reorganization, Neck pain

Neurosurgery 84:588–598, 2019

DOI:10.1093/neuros/nyy066

www.neurosurgery-online.com

Degenerative cervical myelopathy (DCM)¹ is an age-related degenerative condition of the cervical spine and the most common cause of spinal cord dysfunction in elderly individuals.² Many patients with

DCM also experience neck pain that adversely affects their quality of life.^{3,4} Conventional cervical spine imaging has shown inconsistent correlation with neurological symptoms and limited predictive power in determining surgical outcomes.^{5–7} Thus, there remains a critical gap in our knowledge base regarding the development of neurological symptomatology in patients with DCM, which often occurs as a result of advanced compression of the spinal cord from cervical spondylosis (CS). A better understanding of the impact of this and other types of spinal cord injury (SCI) on the entire central nervous system as a unit is desperately needed, and may help bridge our current knowledge gaps.

Laboratory^{8,9} and clinical studies^{10–14} have demonstrated that SCI can induce deleterious

ABBREVIATIONS: 3-D, 3-dimensional; ACC, anterior cingulate cortex; BA, Brodmann area; CS, cervical spondylosis; DCM, degenerative cervical myelopathy; DLPFC, dorsolateral prefrontal cortex; HC, healthy control; mJOA, modified Japanese Orthopedic Association; MRI, magnetic resonance imaging; NDI, Neck Disability Index; SCI, spinal cord injury; VIF, variance inflation factor

Supplemental digital content is available for this article at www.neurosurgery-online.com.

cortical alterations ranging from atrophy of projecting neurons to cell death. Investigations by Freund et al^{13,14} and Hou et al¹² demonstrated that SCI patients had significant cortical atrophy in the primary motor and sensory regions, and that the degree of gray matter loss correlated to functional status. The significance of these findings, and a major rationale for this line of study, is that permanent structural changes in the brain could serve as a potential barrier to clinical recovery in spite of repair of the local injury site.¹¹

Previous investigations regarding the supraspinal alterations that occur during the pathogenesis of DCM have been more focused on the functional brain alterations associated with this disorder,^{15,16} rather than assessing structural changes. In the present study, we seek to probe sensorimotor networks for structural cortical and subcortical changes related to SCI and its relationship with neurological impairment.

Additionally, neck pain has been largely understudied in CS patients. Brain imaging studies in patients with other chronic pain conditions have reported extensive structural and functional changes.¹⁷⁻²³ Together, these studies have helped establish a conceptual framework for a common “pain matrix,” including regions of the thalamus, insular cortex, cingulate cortex, and the dorsolateral prefrontal cortex (DLPFC),^{17,24} consistent with a maladaptive response to recurring pain. Another goal of this investigation was to obtain a better understanding of the supraspinal response to neck pain that may occur in patients with CS.

METHODS

Patient Population

A total of 26 CS patients with or without myelopathy were prospectively enrolled in this cross-sectional study involving observational magnetic resonance imaging (MRI) and evaluation of neurological function. Patients were recruited from an outpatient neurosurgery clinic, and each had at least moderate cervical stenosis on standard cervical MRI. Patients with any additional neurological conditions, such as multiple sclerosis, were excluded from this study. All patients signed Institutional Review Board approved consent forms, and all analyses were done in compliance with the Health Insurance Portability and Accountability Act. The cohort included 20 males and 6 females, with a mean age of 59 yr (range 40-80). The modified Japanese Orthopedic Association (mJOA) score was used as a measure of neurological function.²⁵ The mean mJOA score for the patient cohort was 15 (range 9-18). Of the 26 patients, 6 had neck pain only without neurological symptomatology (mJOA = 18), 14 presented with mild myelopathy (mJOA of 15-17), and 6 presented with moderate to severe myelopathy (mJOA < 14). The Neck Disability Index (NDI) was used as a measure of neck pain and disability.^{26,27} Of the 26 patients enrolled in this study, 23 had NDI scores (nonpercentage scale, range 0-37): 8 had no disability (0-4), 10 had mild disability (5-14), 1 had moderate disability (15-24), 1 had severe disability (25-34), and 2 had complete disability (35-50). A cohort of 17 neurologically intact, healthy volunteer subjects (11 males and 6 females with average age of 40 yr, range 25-62) underwent the same MRI protocol for comparison. MRI data from an additional 28 healthy control (HC) subjects (21 males and 7 females) older than age 40 yr and similar T1 scans were extracted

from the Pain and Interoception Imaging Network (PAIN) Repository, (<http://uclacns.org/programs/pain-research-program/pain-repository/>) maintained by the Center for the Neurobiology of Stress and Resilience.²⁸ Neurological disease was an exclusionary factor for the HC group. The HC group had a significantly lower mean age (46) compared to the patient group (59, 2-sided *t*-test, *P* < .001), but age was accounted for as a covariate in the analyses. Patients did not significantly differ from controls in terms of body mass index (BMI, *t*-test, *P* = .4) or sex (Chi-squared test, *P* = .2). CS and HC demographics are summarized in Table 1.

MRI Acquisition

High-resolution 3-dimensional (3-D) T1-weighted structural MRIs were acquired on a 3T MR scanner (Siemens Prisma or Trio; Siemens Healthcare, Erlangen, Germany) using a 3-D magnetization-prepared rapid gradient-echo sequence in either the coronal, sagittal, or axial orientation, a repetition time (TR) of 2300 to 2500 ms, an echo time (TE) of 2 to 3 ms, an inversion time (TI) of 900 to 945 ms, a flip angle of 9°, and a field of view and matrix size chosen for 1 mm³ isotropic voxel size. CS patients also underwent routine clinical MRI of the spine, including T2w anatomic axial and sagittal scans, which were used to measure the anterior-posterior spinal canal diameter at the site with the largest extent of compression to obtain an MRI version of the Torg-Pavlov ratio,²⁹ and to record the presence of T2 hyperintensity in the spinal cord.

Image Processing and Analysis

Cortical segmentation and computation of cortical thickness was performed using FreeSurfer (<https://surfer.nmr.mgh.harvard.edu/fswiki>)³⁰⁻³² on the T1 images. Processed brain surfaces were smoothed with a full-width half-maximum of 10 mm then registered to a standard space. Evaluation of the associations of neuroimaging measures with mJOA scores were performed in the combined group of HC subjects and CS patients. When examining NDI, HC subjects were excluded from analyses. Age, which has a predominantly linear relation to cortical thickness,³²⁻³⁴ was included as a covariate in analyses. The vertex-wise level of significance was set at *P* < .05, with multiple comparisons correction performed by using Monte Carlo permutations³⁵ with a significance level of *P* < .05.

Multiple linear regression analyses were performed for symptom variables, age, and neuroimaging measures, which yielded significance (*P*-value) for each variable in the model, as well as the goodness-of-fit for the model (fraction of variance explained, *R*²) and goodness-of-fit adjusted for multiple variables (adjusted *R*²).^{36,37} Multiple linear regression was performed for cortical thickness in regions identified by FreeSurfer analysis and defined by the Desikan-Killiany-Tourville (DKT) atlas.³⁸ Additionally, we analyzed pre- and postcentral gyrii in relation to mJOA, and anterior cingulate cortex (ACC), insular cortex, and rostral middle frontal gyrus (equivalent to the DLPFC) in relation to NDI. The volume of the subcortical regions of the thalamus, caudate, putamen, and pallidum³⁹ were also evaluated via multiple linear regression for both mJOA and NDI. To ensure the appropriateness of multiple linear regression models, we computed variance inflation factors (VIF) for age and symptom measure, Goldfeld-Quandt tests for Heteroskedasticity⁴⁰ at type-I error-corrected rate of 0.05, and D'Agostino & Pearson normality tests for the residuals.⁴¹ Regressions which did not pass these tests were discarded. We also performed an exploratory analysis of the motor and sensory strips by quantifying thickness on the unsmoothed brain surfaces in sequential 10 mm

TABLE 1. CS Patients and HC Subjects Cohort Demographics

Subject Population	n	Age (mean years \pm SD)	Sex	BMI (mean \pm SD)	mJOA (mean \pm SD)	NDI (mean \pm SD)
CS Patients	26	59 \pm 11 years	20M/6F	27.2 \pm 6.7	15.4 \pm 2.8	10.6 \pm 10
HC Volunteers	45	46 \pm 10 years	32M/13F	26.2 \pm 4.8	18	

segments along the primary motor and primary sensory Brodmann areas (BAs) (Figure, Supplemental Digital Content 1).⁴² We computed 2-way ANOVAs for each BA with group and segment distance as factors, and Pearson's correlation coefficients between thickness and mJOA (for combined CS and HC group) and NDI (for subset of CS group with NDI scores) at each segment. Both the 2-way ANOVAs and Pearson's correlations computations employed Sidak-Holm^{43,44} multiple comparisons correction. Regional, as well as whole-brain, mean cortical thickness with age regressions were also performed in order to compare age-related changes in brain structure for CS patients and HC subjects. All analyses were performed using FreeSurfer (Version 5.3.0, <https://surfer.nmr.mgh.harvard.edu/fswiki>), GraphPad Prism (Version 7.0b, La Jolla, California, www.graphpad.com), and multiple regression was performed in Free Statistics Software (Version 1.1.23-r7, http://www.wessa.net/rwasp_multipleregression.wasp/).

RESULTS

Conventional Clinical Spine MRI Findings

The mean anterior-posterior spinal canal diameter at the site of the largest extent of compression was 6.1 mm (\pm 1.6 mm standard deviation, range 3.7-10.3 mm), and the mean MRI equivalent of the Torg-Pavlov ratio was 0.36 (\pm 0.10 standard deviation, range 0.20-0.58) in the cohort of CS patients. Out of the 26 CS patients, 14 (54%) presented with T2 hyperintensity within the cord. Linear regression indicated that neither spinal canal diameter nor MRI-equivalent Torg-Pavlov were correlated with neurological function (mJOA, $R^2 = 0.092$, $P = .1$, and $R^2 = 0.050$, $P = .3$, respectively) or neck pain (NDI, $R^2 < 0.0001$, $P > .9$, and $R^2 = 0.0008$, $P = .7$, respectively). Subjects with T2 hyperintensity in the spinal cord did not have a significantly different mJOA from those without (t -test, $P = .7$), but did present with significantly lower NDI (t -test, $P = .01$).

Association Between Cortical Thickness, Subcortical Volume, and Neurological Function

Results from the current study demonstrate decreasing cortical thickness in several brain regions with increasing neurological deficits and pain severity while accounting for age. Figure 1 highlights results from vertex-wise correlations with mJOA score, for which there were significantly positively correlated regions (decreasing cortical thickness with decreasing mJOA, ie, worse neurological score) within the precuneus bilaterally (Figure 1; Region 1a, left; Region 1d, right), in the left superior frontal lobe (Figure 1; Region 1b), and in a region extending across the right superior frontal lobe and the right caudal anterior cingulate (Figure 1; Region 1c). The VIF for age and mJOA in

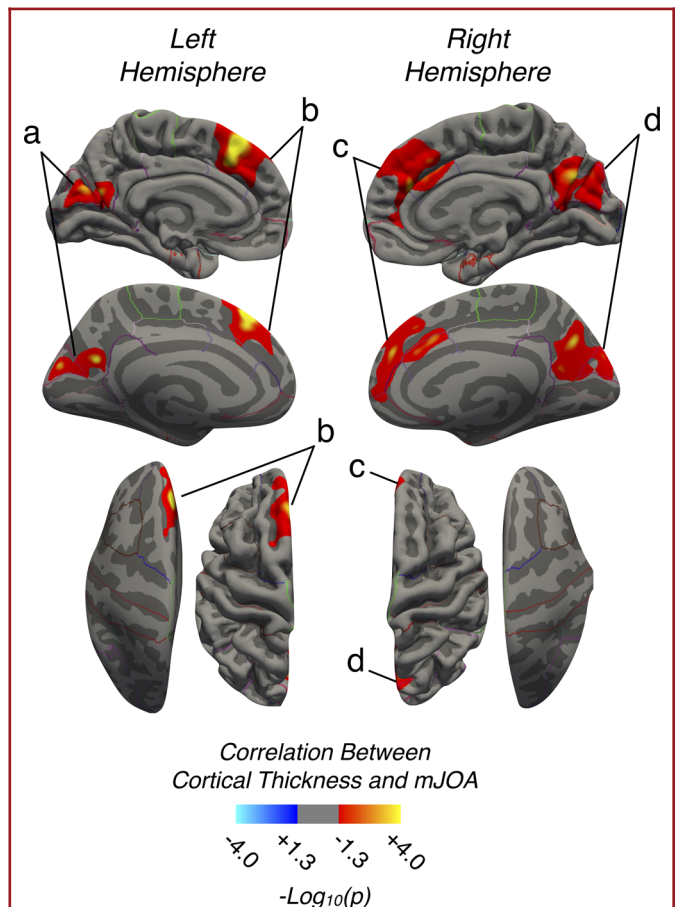


FIGURE 1. Regions demonstrating a strong association between cortical thickness and mJOA in CS patients and HC subjects. Red-Yellow denotes increasing cortical thickness with increasing mJOA score (better neurological function). Regions with significant associations were identified in the a, left precuneus and cuneus; b, left superior frontal lobe; c, right superior frontal lobe extending into the anterior cingulate; and d, right precuneus and cuneus.

the multiple linear regressions was 1.14, and cortical thickness within the precuneus, left superior frontal lobe, caudal anterior caudate, and pre- and postcentral gyri resulted in an observed association with both mJOA and age (Table 2). The right superior frontal lobe presented with a significant association but failed tests for heteroskedasticity and normality of residuals. In addition to the cortical regions, we observed a significant positive association between the volume of the putamen and both mJOA and

TABLE 2. Multiple Linear Regression of Mean Cortical Thickness and Subcortical Volume with mJOA and Age

Measure	Region	mJOA	mJOA P-Value	Age	Age P-Value	R ²	Adj. R ²	Overall Model P-Value
Cortical Thickness	LH Precuneus	0.019	.04	−0.0045	.005	0.2214	0.1988	<.001
	LH Sup. Frontal	0.020	.04	−0.0030	.09	0.1403	0.115	.006
	RH Precuneus	0.032	.001	−0.005	.001	0.3418	0.3224	<.001
Subcortical Volume	LH Putamen	145	<.001	−36	<.001	0.4483	0.4321	<.001
	RH Putamen	130	<.001	−35	<.001	0.4903	0.4753	<.001

LH and RH are left and right hemisphere, Sup. denotes Superior.

age (Multiple Linear Regression, $R^2 = 0.4483$ for the left, and $R^2 = 0.4903$ for the right putamen).

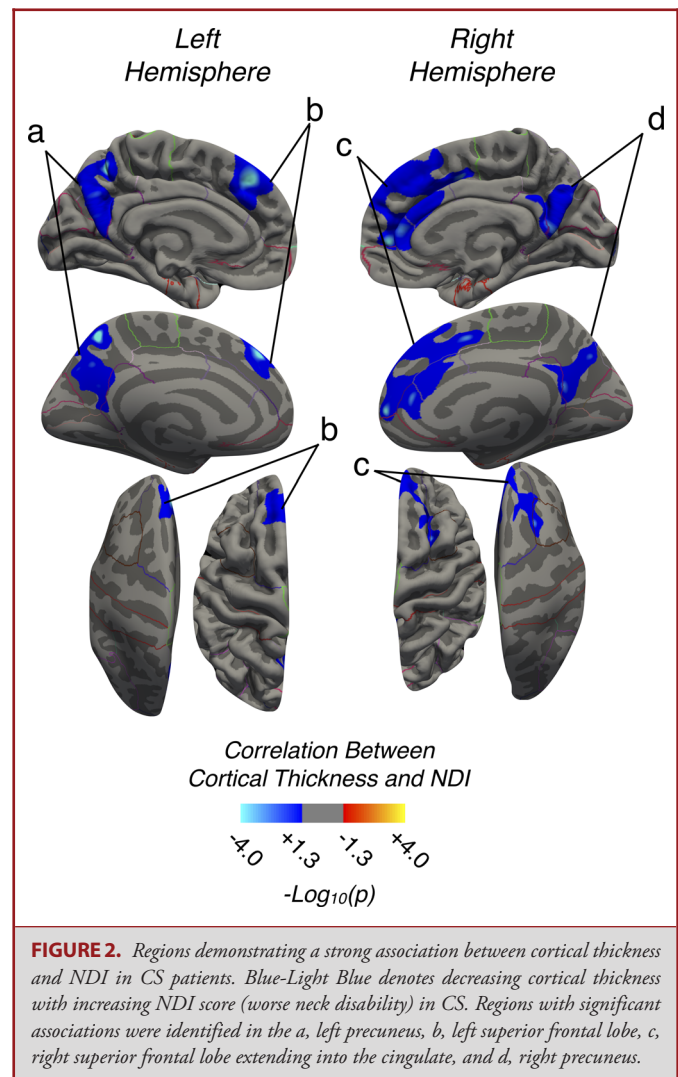
Examination of patients with CS exclusively ($n = 26$; excluding HCs) uncovered similar reductions in cortical thickness within the superior frontal lobe, but thinning within the precuneus was no longer associated with decreased mJOA score (Figure, Supplemental Digital Content 2). Multiple linear regression (Table, Supplemental Digital Content 3) only confirmed the association between the reduction in the volume of the left and right putamen and mJOA ($P = .03$ and $P = .01$, respectively), though the left and right precuneus were trending towards significance ($P = .1$ and $P = .06$, respectively, VIF for age and mJOA of 1.14).

Association Between Cortical Thickness, Subcortical Volume, and Neck Pain

Consistent with trends observed in overall neurological status, results demonstrated a significant association between cortical thickness and NDI while accounting for age, as illustrated in Figure 2. We observed a decreasing cortical thickness with increasing NDI (ie, worse neck pain) in the left and right precuneus (Figure 2; Regions 2a and 2d), as well as the left superior frontal lobe (Figure 2; Region 2b), and a region extending across the superior frontal and portions of the right ACC (Figure 2; Region 2c). The VIF for age and mJOA in the multiple linear regressions was 1.12, and bilateral regions of the precuneus, right insula, right superior frontal gyrus, and the right caudal anterior cingulate were all found to be associated with NDI (Table 3). The right rostral anterior cingulate failed the test for normality of residuals.

Changes in Primary Sensory and Motor Cortical Thickness

Examination of cortical thickness across sensory and motor strips indicated a moderate but significant association between thickness in BA3a and mJOA at multiple segments as well as greater mean difference in cortical thickness between CS and HC groups (Figure 3 for sensory; and Figure 4 for motor). Both primary motor areas examined (BA4a and BA4p, Figure 4A and Figure 4B, respectively) demonstrated spatially varying moderate but significant relationships between mJOA scores and mean cortical thickness, though generally there was no significant differ-



ences between CS and HC groups. When looking at the group factor for the 2-way ANOVA, most BAs showed a significant group effect, meaning that while the differences at each segment were small the general trend for lower thickness across the region in CS patients was still significant. For NDI, correlations failed to

TABLE 3. Multiple Linear Regressions of Mean Cortical Thickness and Subcortical Volume with NDI and Age

Measure	Region	NDI	NDI P-Value	Age	Age P-Value	R ²	Adj. R ²	Overall Model P-Value
Cortical Thickness	LH Precuneus	-0.012	<.001	-0.014	<.001	0.5934	0.5528	<.001
	LH Insula	-0.0095	.01	-0.018	<.001	0.6098	0.5708	<.001
	RH Caud. Ant. Cingulate	-0.021	.003	0.0007	.9	0.3954	0.3349	.007
	RH Precuneus	-0.012	<.001	-0.013	<.001	0.5739	0.5313	<.001
	RH Sup. Frontal	-0.012	.004	-0.0041	.3	0.3524	0.2877	.01
Subcortical Volume	LH Putamen	-36	.01	-54	<.001	0.5122	0.4634	<.001
	RH Putamen	-38	<.001	-45	.001	0.5856	0.5441	<.001

LH and RH are left and right hemisphere, Sup. denotes Superior, Rost. denotes Rostral, Ant. denotes Anterior.

reach statistical significance, potentially due to lack of statistical power from a smaller cohort of subjects with NDI scores.

Age-Related Changes in Cortical Thickness Between CS and HCs

Lastly, CS patients demonstrated a greater degree of cortical thinning with age (Figure 5). Both the left postcentral gyrus ($P = .016$) and precuneus ($P = .028$) showed a faster rate of thinning. Additionally, the left and right putamen ($P = .002$ and $P = .008$, respectively) and the right precuneus ($P = .009$) showed lower mean cortical thickness values in CS patients compared to HC subjects. For whole-brain mean cortical thickness, CS patients had a faster rate of thinning (loss of 0.0069 mm/yr) than HC (loss of 0.0036 mm/yr), and though not statistically significant, the HC rate was comparable to the loss of 0.004 mm/yr reported in a larger study by Lemaitre et al.³³

DISCUSSION

SCI and Brain Changes

Recent studies have demonstrated that SCI can induce atrophic alterations of the supraspinal neural network, and that the extent of these changes can correlate with degree of neurological impairment. Hou et al¹² found in SCI patients that gray matter volume reduction in the primary motor cortex significantly correlated with the American Spinal Injury Association motor score. Using voxel-based morphometry, Freund et al¹⁴ determined that spinal cord atrophy following SCI was significantly correlated with degree of cortical atrophy. Moreover, in a separate study, Freund et al¹³ established that SCI patients that had lower volume change of the corticospinal tract at the level of the internal capsule had a significantly better neurological outcome than those with a higher volume loss. These investigations highlight some of the upstream adaptations within the sensorimotor network that occur following traumatic SCI and their potential impact on both functional status and recovery.

Comparatively less is known about the supraspinal alterations that occur as a result of chronic SCI associated with cervical disc disease. Unique patterns of task-based functional MRI activation have been observed in DCM patients, who exhibited larger

areas of activation during simple motor tasks when compared to HC subjects.^{15,16} After surgery, these same patients displayed a smaller area of activation which correlated with neurological improvement, and was comparable to the area of activation for the same task in HC subjects.^{15,16} As with acute traumatic SCI patients, it is believed that this recruitment of other cortical areas is a compensatory mechanism designed to maintain neurological function in the face of diminished efferent and afferent connections.

Results from the current study support the hypothesis that chronic SCI related to cervical stenosis results in specific structural changes within the brain. CS patients displayed a consistent pattern of brain changes with associated clinical symptoms of both neurological function (mJOA) and neck pain (NDI), namely decreases in cortical thickness within precuneus and superior frontal regions, and decreased volume of the putamen. We also observed cortical thinning in the anterior cingulate and insula, and increasing atrophy within BA3a and in primary motor regions with worsening neurological symptom severity. Patients with CS also displayed a faster rate of cortical thinning and atrophy with age compared to HC subjects. These are critically important findings, and could potentially have an impact on the understanding of the pathogenesis of DCM and recovery following surgical intervention.

Primary Sensorimotor Reorganization with Neurological Symptoms

The association between decreased cortical thickness within BA3a and increasing neurological symptom severity is consistent with the role of BA3a in receiving afferent information regarding proprioception and motor actions,⁴⁵ as CS patients with myelopathy are known to have deficits in proprioception⁴⁶ relating to both gait⁴⁷ and hand function.⁴⁸ While cortical thickness in the precentral gyrus, in general, was not associated with neurological impairment, subdivisions of the motor strip (BA4a and BA4p) appeared associated with changes in mJOA. This lack of widespread changes in the precentral gyrus across all patients likely reflects the variability in specific motor deficits across patients (ie, upper or lower extremity deficits) and their relation to reorganization within the motor cortex.

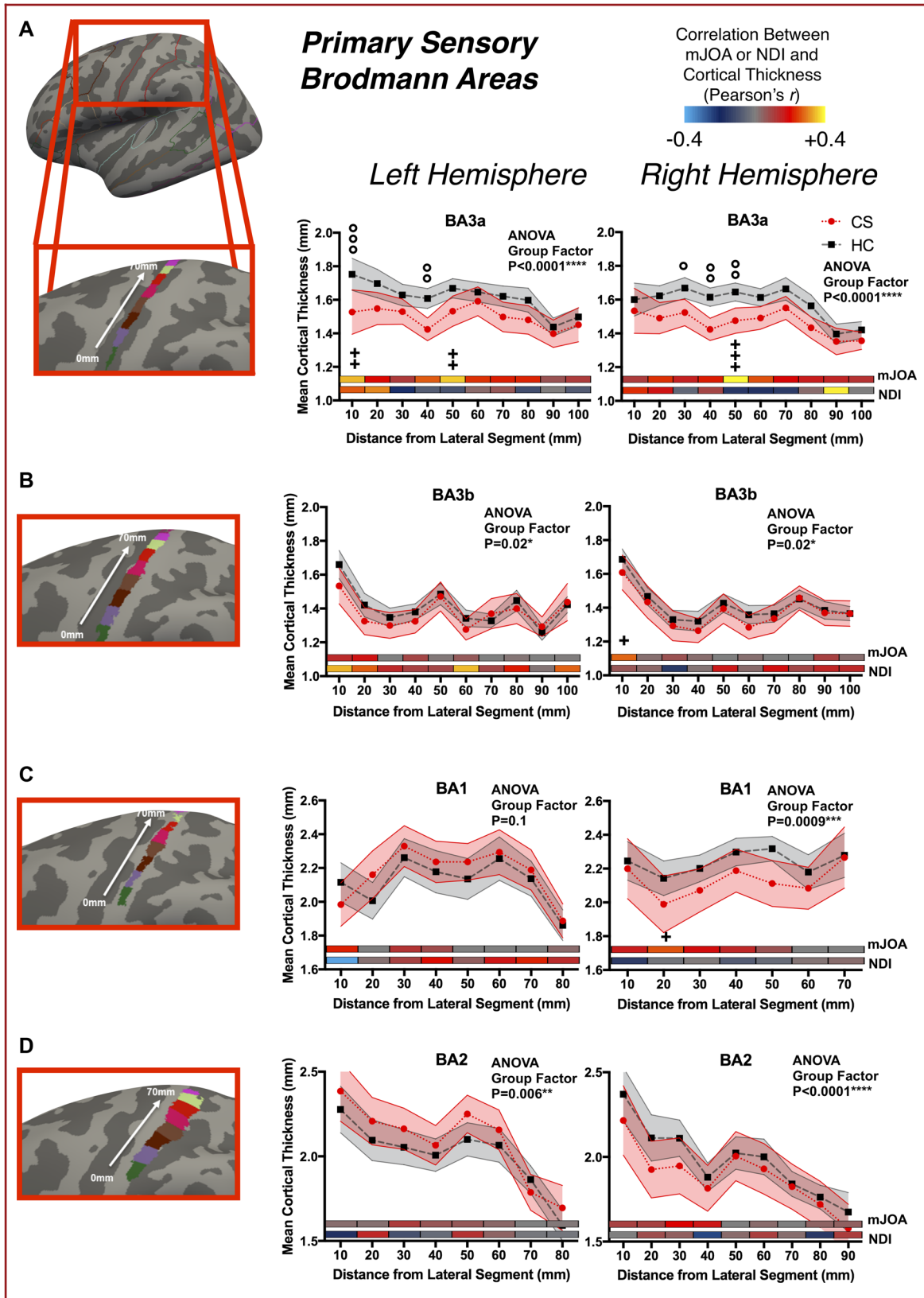


FIGURE 3. Cortical thickness as a function of distance in 1 cm segments across primary sensory Brodmann areas (BAs), including **A**, BA3a; **B**, BA3b; **C**, BA1; and **D**, BA2. Values in plot reflect mean and 95% confidence intervals for CS patients and HC subjects. The x-axis is distance from first segment, laterally to medially as illustrated on the figures to the left, the y-axis is cortical thickness, and plotted are the mean values for each group. Displayed within each plot is the color-coded Pearson correlation coefficient for the mJOA and NDI scores with the mean cortical thickness in each segment. For each BA, the P-value for the Group Effect in the 2-way ANOVA (group and distance) is displayed. Significance after Sidak-Holm correction is shown for group differences (displayed above plotted values for the groups, denoted by the '°' symbol) and Pearson's correlation with mJOA (displayed below the plotted values for the groups and above the color-coded bars, denoted by the '+' symbol); Pearson's correlations with NDI showed no significant results.

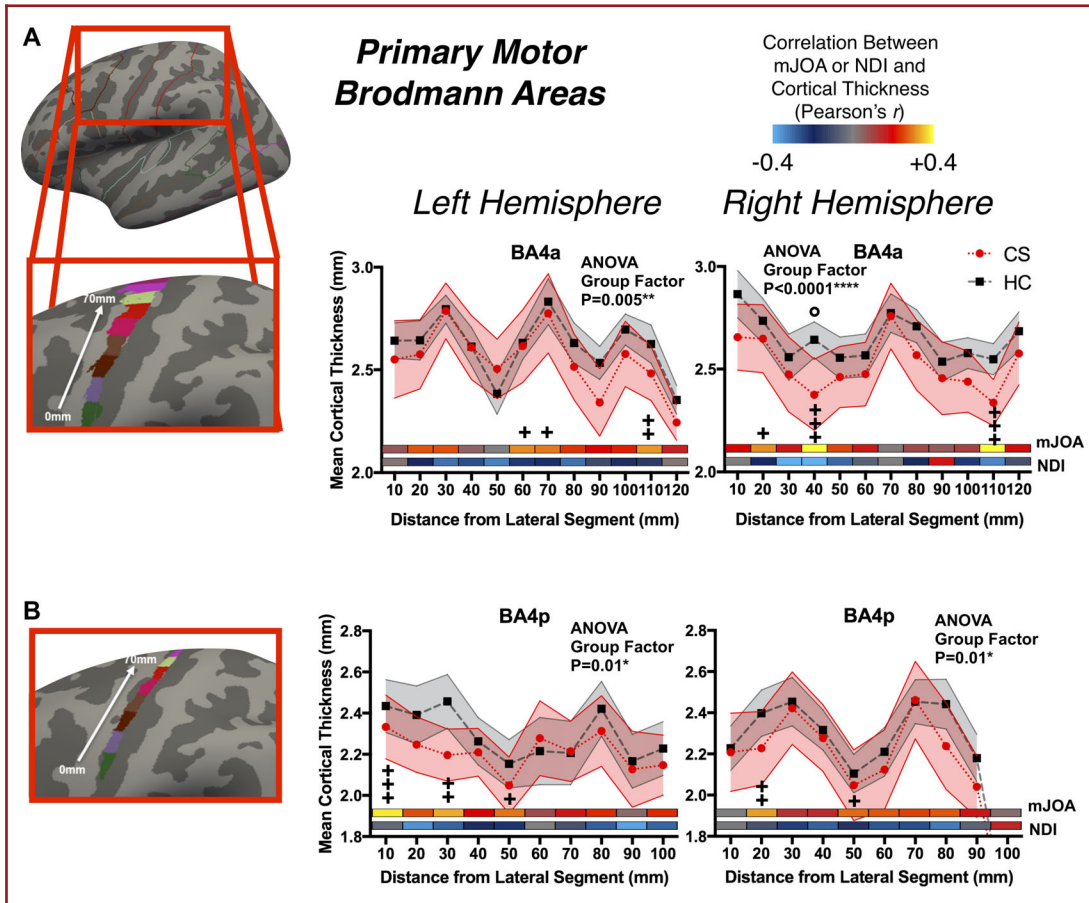
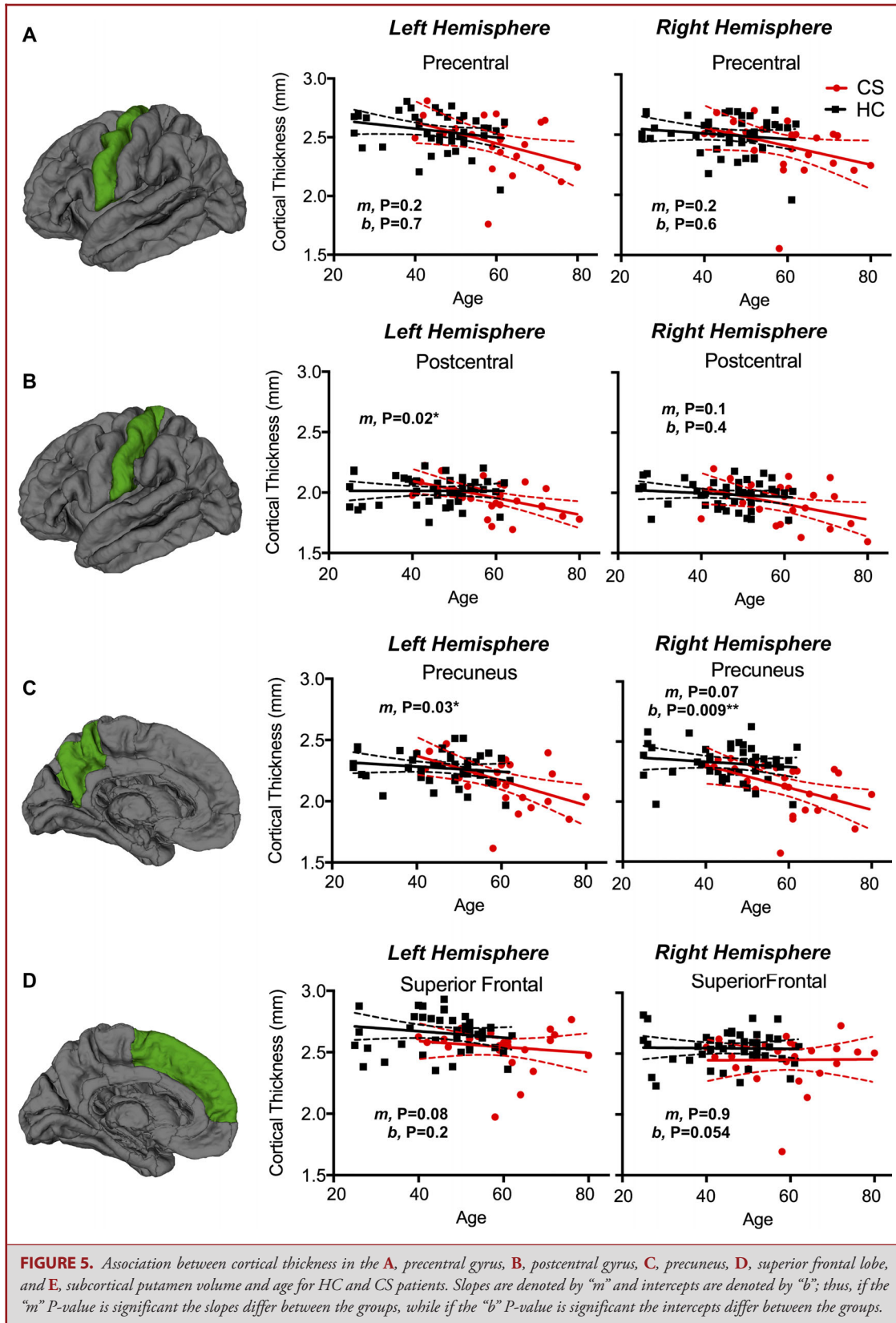


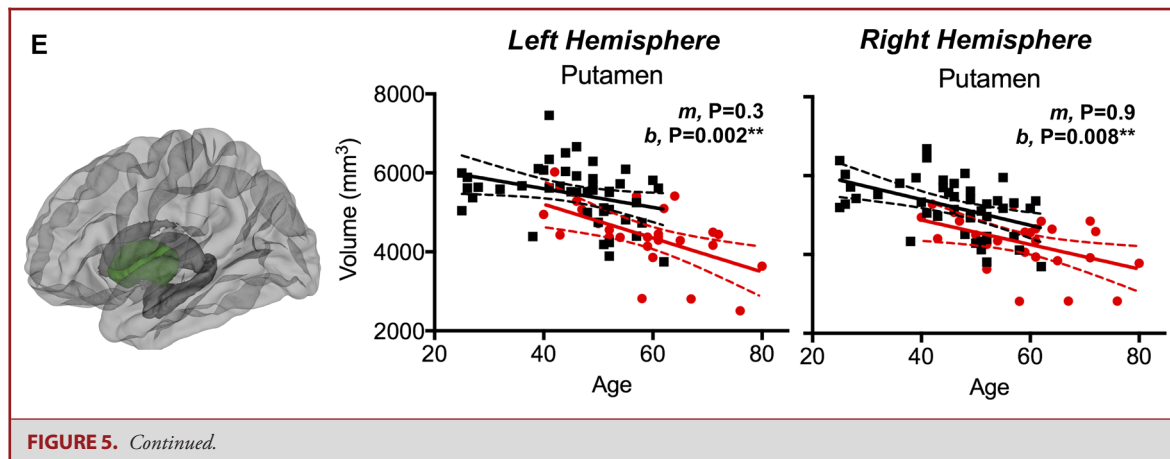
FIGURE 4. Cortical thickness as a function of distance in 1 cm segments across primary motor BA, including **A**, BA4a and **B**, BA4p. Values in plot reflect mean and 95% confidence intervals for CS patients and HC subjects. The x-axis is distance from first segment, laterally to medially as illustrated on the figures to the left, the y-axis is cortical thickness, and plotted are the mean values for each group. Displayed within each plot is the color-coded Pearson correlation coefficient for the mJOA and NDI scores with the mean cortical thickness in each segment. For each BA, the P-value for the Group Effect in the 2-way ANOVA (group and distance) is displayed. Significance after Sidak-Holm correction is shown for group differences (displayed above plotted values for the groups, denoted by the '°' symbol) and Pearson's correlation with mJOA (displayed below the plotted values for the groups and above the color-coded bars, denoted by the '+' symbol); Pearson's correlations with NDI showed no significant results.

Structural Brain Changes with Chronic Neck Pain

We hypothesized that CS patients would exhibit similar alterations in brain structure to those observed in other chronic pain conditions. Results from this study confirmed a decrease in cortical thickness within the cingulate and insular cortices

may occur with worsening neck pain, which is consistent with modern theories associated with chronic pain structural reorganization.^{17,24} The ACC is known to be a key area in the central sensitization in chronic pain, potentially acting by long-term potentiation,^{49,50} and a decrease in gray matter within the ACC





has been observed in multiple chronic pain studies.^{51,52} These changes suggest that neck pain exhibited by some patients with CS may alter neural structures involved in the central sensitization of pain.

Limitations

An important limitation of the current study was the age differences between CS and HC subjects. While CS patients had a higher age on average, we accounted for age as a covariate by modeling it as a linear factor, which is justified by many studies involving brain structure and aging.^{32,34} Even when the effects of age were taken into consideration as a covariate, there were a number of statistically significant correlations between both the mJOA and NDI with structural alterations encountered in the CS cohort. Larger studies or studies involving HC subjects with a wider age range are warranted to verify our current observations.

CONCLUSION

Patients with CS appear to display cortical atrophy in specific regions of the brain in association with a wide range of neurological symptom severity. Results support the central hypothesis that widespread alterations in the structure of the neuraxis occur as a result of spinal cord injury. Additionally, results support the notion that, in addition to primary sensorimotor areas, supplemental brain related to the execution of complex movements such as gait, grasp, and fine hand-motor coordination, are also altered in the presence of spinal cord compression. Further studies aimed at verifying our current observations of cortical atrophy as well as determining whether surgical interventions reverse this degeneration are warranted.

Disclosures

Funding was received through the following NIH/NINDS grants: no. 1R21NS065419-01A1 (to L.T.H. and N.S.) and no. 1R01NS078494-01A1 (to L.T.H., N.S., and B.M.E.). The authors have no personal, financial, or institutional interest in any of the drugs, materials, or devices described in this article.

REFERENCES

- Nouri A, Tetreault L, Singh A, Karadimas SK, Fehlings MG. Degenerative cervical myelopathy: epidemiology, genetics, and pathogenesis. *Spine (Phila Pa 1976)*. 2015;40(12):E675-E693.
- Kalsi-Ryan S, Karadimas SK, Fehlings MG. Cervical spondylotic myelopathy: the clinical phenomenon and the current pathobiology of an increasingly prevalent and devastating disorder. *Neuroscientist*. 2013;19(4):409-421.
- Binder AI. Cervical spondylosis and neck pain. *BMJ*. 2007;334(7592):527-531.
- Rao R. Neck pain, cervical radiculopathy, and cervical myelopathy - pathophysiology, natural history, and clinical evaluation. *J Bone Joint Surg Am*. 2002;84a(10):1872-1881.
- Tetreault LA, Dettori JR, Wilson JR, et al. Systematic review of magnetic resonance imaging characteristics that affect treatment decision making and predict clinical outcome in patients with cervical spondylotic myelopathy. *Spine*. 2013;38(22):S89-S110.
- Yue WM, Tan SB, Tan MH, Koh DCS, Tan CT. The Torg-Pavlov ratio in cervical spondylotic myelopathy - a comparative study between patients with cervical spondylotic myelopathy and non-spondylotic, nonmyelopathic population. *Spine*. 2001;26(16):1760-1764.
- Mastrorardi L, Elsawaf A, Roperto R, et al. Prognostic relevance of the postoperative evolution of intramedullary spinal cord changes in signal intensity on magnetic resonance imaging after anterior decompression for cervical spondylotic myelopathy. *J Neurosurg Spine*. 2007;7(6):615-622.
- Hains BC, Black JA, Waxman SG. Primary cortical motor neurons undergo apoptosis after axotomizing spinal cord injury. *J Comp Neurol*. 2003;462(3):328-341.
- Barron KD, Dentinger MP, Popp AJ, Mankes R. Neurons of layer Vb of rat sensorimotor cortex atrophy but do not die after thoracic cord transection. *J Neuropathol Exp Neurol*. 1988;47(1):62-74.
- Jurkiewicz MT, Crawley AP, Verrier MC, Fehlings MG, Mikulis DJ. Somatosensory cortical atrophy after spinal cord injury: a voxel-based morphometry study. *Neurology*. 2006;66(5):762-764.
- Wrigley PJ, Gustin SM, Macey PM, et al. Anatomical changes in human motor cortex and motor pathways following complete thoracic spinal cord injury. *Cereb Cortex*. 2009;19(1):224-232.
- Hou JM, Yan RB, Xiang ZM, et al. Brain sensorimotor system atrophy during the early stage of spinal cord injury in humans. *Neuroscience*. 2014;266:208-215.
- Freund P, Weiskopf N, Ashburner J, et al. MRI investigation of the sensorimotor cortex and the corticospinal tract after acute spinal cord injury: a prospective longitudinal study. *Lancet Neurol*. 2013;12(9):873-881.
- Freund P, Weiskopf N, Ward NS, et al. Disability, atrophy and cortical reorganization following spinal cord injury. *Brain*. 2011;134(6):1610-1622.
- Dong Y, Holly LT, Albigestui-Dubois R, et al. Compensatory cerebral adaptations before and evolving changes after surgical decompression in cervical spondylotic myelopathy. *J Neurosurg Spine*. 2008;9(6):538-551.

16. Holly LT, Dong Y, Albistegui-DuBois R, Marehbian J, Dobkin B. Cortical reorganization in patients with cervical spondylotic myelopathy. *J Neurosurg Spine*. 2007;6(6):544-551.
17. Apkarian AV, Hashmi JA, Baliki MN. Pain and the brain: specificity and plasticity of the brain in clinical chronic pain. *Pain*. 2011;152(Supplement):S49-S64.
18. May A. Chronic pain may change the structure of the brain. *Pain*. 2008;137(1):7-15.
19. Apkarian AV, Baliki MN, Geha PY. Towards a theory of chronic pain. *Prog Neurobiol*. 2009;87(2):81-97.
20. Ivo R, Nicklas A, Dargel J, et al. Brain structural and psychometric alterations in chronic low back pain. *Eur Spine J*. 2013;22(9):1958-1964.
21. Davis KD, Pope G, Chen J, Kwan CL, Crawley AP, Diamant NE. Cortical thinning in IBS: implications for homeostatic, attention, and pain processing. *Neurology*. 2008;70(2):153-154.
22. Frokjaer JB, Bouwense SAW, Olesen SS, et al. Reduced cortical thickness of brain areas involved in pain processing in patients with chronic pancreatitis. *Clin Gastroenterol Hepatol*. 2012;10(4):434.e1-438.e1.
23. Cauda F, Palermo S, Costa T, et al. Gray matter alterations in chronic pain: a network-oriented meta-analytic approach. *NeuroImage*. 2014;4:676-686.
24. Apkarian AV. The Brain Adapting With Pain: Contribution of Neuroimaging Technology to Pain Mechanisms. Philadelphia: Wolters Kluwer; 2015.
25. Yonenobu K, Abumi K, Nagata K, Taketomi E, Ueyama K. Interobserver and intraobserver reliability of the Japanese orthopaedic association scoring system for evaluation of cervical compression myelopathy. *Spine (Phila Pa 1976)*. 2001;26(17):1890-1894; discussion 1895.
26. Vernon H. The Neck Disability Index: State-of-the-Art, 1991-2008. *J Manipulative Physiol Ther*. 2008;31(7):491-502.
27. Vernon H, Mior S. The Neck Disability Index: a study of reliability and validity. *J Manipulative Physiol Ther*. 1991;14(7):409-415.
28. Labus JS, Naliboff B, Kilpatrick L, et al. Pain and Interoception Imaging Network (PAIN): a multimodal, multisite, brain-imaging repository for chronic somatic and visceral pain disorders. *Neuroimage*. 2016;124(Pt B):1232-1237.
29. Pavlov H, Torg JS, Robie B, Jahre C. Cervical spinal stenosis: determination with vertebral body ratio method. *Radiology*. 1987;164(3):771-775.
30. Dale AM, Fischl B, Sereno MI. Cortical surface-based analysis. *Neuroimage*. 1999;9(2):179-194.
31. Fischl B, Dale AM. Measuring the thickness of the human cerebral cortex from magnetic resonance images. *P Natl Acad Sci USA*. 2000;97(20):11050-11055.
32. Salat DH, Buckner RL, Snyder AZ, et al. Thinning of the cerebral cortex in aging. *Cereb Cortex*. 2004;14(7):721-730.
33. Lemaitre H, Goldman AL, Sambataro F, et al. Normal age-related brain morphometric changes: nonuniformity across cortical thickness, surface area and gray matter volume? *Neurobiol Aging*. 2012;33(3):617.e1-617.e9.
34. Sowell ER, Peterson BS, Kan E, et al. Sex differences in cortical thickness mapped in 176 healthy individuals between 7 and 87 years of age. *Cereb Cortex*. 2007;17(7):1550-1560.
35. Hagler DJ, Saygin AP, Sereno MI. Smoothing and cluster thresholding for cortical surface-based group analysis of fMRI data. *Neuroimage*. 2006;33(4):1093-1103.
36. Lai TL, Robbins H, Wei CZ. Strong consistency of least squares estimates in multiple regression II. *J Multivariate Anal*. 1979;9(3):343-361.
37. Lai TL, Robbins H, Wei CZ. Strong consistency of least squares estimates in multiple regression. *P Natl Acad Sci USA*. 1978;75(7):3034-3036.
38. Klein A, Tourville J. 101 labeled brain images and a consistent human cortical labeling protocol. *Front Neurosci*. 2012;6:171.
39. Fischl B, Salat DH, Busa E, et al. Whole brain segmentation: automated labeling of neuroanatomical structures in the human brain. *Neuron*. 2002;33(3):341-355.
40. Goldfeld SM, Quandt RE. Some tests for homoscedasticity. *J Am Statist Assoc*. 1965;60(310):539-547.
41. D'Agostino RB. Tests for the normal distribution. In: *Goodness-of-Fit Techniques*, vol. 68. 1986:576.
42. Fischl B, Rajendran N, Busa E, et al. Cortical folding patterns and predicting cytoarchitecture. *Cereb Cortex*. 2008;18(8):1973-1980.
43. Holm S. A simple sequentially rejective multiple test procedure. *Scand J Stat*. 1979;6(2):65-70.
44. Seaman MA, Levin JR, Serlin RC. New developments in pairwise multiple comparisons: some powerful and practicable procedures. *Psychol Bull*. 1991;110(3):577-586.
45. Patestas MA, Gartner LP. *A Textbook of Neuroanatomy*. Malden, MA: Blackwell; 2006.
46. Harrop JS, Hanna A, Silva MT, Sharan A. Neurological manifestations of cervical spondylosis: an overview of signs, symptoms, and pathophysiology. *Neurosurgery*. 2007;60(1 suppl 1):S14-S20.
47. Nardone A, Galante M, Grasso M, Schieppati M. Stance ataxia and delayed leg muscle responses to postural perturbations in cervical spondylotic myelopathy. *J Rehabil Med*. 2008;40(7):539-547.
48. Doita M, Sakai H, Harada T, et al. The influence of proprioceptive impairment on hand function in patients with cervical myelopathy. *Spine (Phila Pa 1976)*. 2006;31(14):1580-1584.
49. Zhuo M. Long-term potentiation in the anterior cingulate cortex and chronic pain. *Philos T R Soc B*. 2013;369(1633):20130146-20130146.
50. Bliss TVP, Collingridge GL, Kaang BK, Zhuo M. Synaptic plasticity in the anterior cingulate cortex in acute and chronic pain. *Nat Rev Neurosci*. 2016;17(8):485-496.
51. Rodriguez-Raecke R, Niemeier A, Ihle K, Ruether W, May A. Brain gray matter decrease in chronic pain is the consequence and not the cause of pain. *J Neurosci*. 2009;29(44):13746-13750.
52. Burgmer M, Gaubitz M, Konrad C, et al. Decreased gray matter volumes in the cingulo-frontal cortex and the amygdala in patients with fibromyalgia. *Psychosom Med*. 2009;71(5):566-573.

Supplemental digital content is available for this article at www.neurosurgery-online.com.

Supplemental Digital Content 1. Figure. Processing details for estimating cortical thickness along 10 mm segments of the motor and sensory strips. First, the coordinates of the bilateral Brodmann areas 3a, 3b, 1, 2, 4a, and 4p provided in the FreeSurfer package **A**, were imported into MATLAB (MATLAB Version 2014a, <https://www.mathworks.com/>). **B**, Once imported into MATLAB, the points were collapsed onto both the 2-dimensional (2-D) plane of their x- and y-components and onto the 2-D plane of their x- and z-components, and LOWESS regression with a smoothing window of 10 was used to compute a representative line in x-y and x-z planes. Then the y- and z-components were combined with the x-coordinates to form a representative line in 3-D space. **C**, The line was defined as starting at the most lateral portion along x-, and every 10 mm along the length of the line in 3-D space a plane perpendicular to the line was computed and the points that were within 2 consecutive planes were defined as one 10 mm segment. **D**, Lastly, the 10 mm segments for each BA were imported to FreeSurfer and used to extract mean cortical thickness measures for each subject using their unsmoothed registered cortical surfaces.

Supplemental Digital Content 2. Figure. Regions demonstrating a strong association between cortical thickness and mJOA in group patients with CS only. Red-Yellow denotes increasing cortical thickness with increasing mJOA score (better neurological function). Regions with significant associations were identified in the **A**, left superior frontal lobe, **B**, right superior frontal lobe extending into the anterior cingulate.

Supplemental Digital Content 3. Table. Multiple linear regression of cortical thickness and subcortical volume with mJOA and age, in the CS group only. LH and RH are left and right hemisphere, Sup. is Superior.

COMMENT

This is a prospective cross-sectional study examining structural reorganization in the supraspinal neural network following chronic spinal cord compression. Specifically, the authors looked for correlations between cortical thickness as well as subcortical volumes on MRI and neurological severity in patients with chronic spinal cord compression due to degenerative cervical myelopathy (DCM). Neurological severity was defined using the mJOA and NDI as measures of neurological

function and neck pain, respectively. The authors observed cortical atrophy in the precuneus and superior frontal regions, as well as the volume of the putamen, with worsening neurological disability and pain. They also observed decreased thickness in the cingulate and insular cortices with poorer NDI score.

Previous work in this area has typically focused on acute spinal cord injury or assessing functional changes (using fMRI) in chronic spinal cord compression rather than structural changes. Therefore, this

study provides important new evidence towards widespread changes in the neural-axis following spinal cord injury. However, the study is not designed to test the hypothesis of correlation between the injury and said changes, which should be explored in the future.

Michael G. Fehlings
Muhammad Akbar
Toronto, Ontario



José Orozco's mural "Epic of American Civilization" is located in the Baker Library at Dartmouth College, where it circumnavigates a reading room pinched at the middle by a service desk. The two wings of the space allowed Orozco to tell a story in 2 parts: one devoted to the roots of ancient America, the other characterizing 20th-century America and post-industrialized society. The sequences in the 2 wings mirror each other at key points within the cycle. This image, "Ancient Human Sacrifice", establishes a point of contrast to its counterpoint in the other wing, "Modern Human Sacrifice", showing the dark side of both historical periods. This panel shows a practice that fulfilled the needs of that time's institutionalized religion, while the modern counterpoint shows the human cost of militaristic nationalism. Image: Jose Clemente Orozco, "Ancient Human Sacrifice". Hood Museum of Art, Dartmouth: Commissioned by the Trustees of Dartmouth College. © 2019 Artists Rights Society (ARS), New York / SOMAAP, Mexico City.